# The Adsorption of Unsymmetrical Spiroalkanedithiols onto Gold Affords Multi-Component Interfaces that Are Homogeneously Mixed at the Molecular Level

**Young-Seok Shon, Seunghwan Lee, Scott S. Perry,* and T. Randall Lee***

*Contribution from the Department of Chemistry, University of Houston, Houston, Texas 77204-5641*

*Received June 14, 1999*

**Abstract:** Exposure of the unsymmetrical spiroalkanedithiol, 2-octyl-2-pentadecylpropane-1,3-dithiol, to the surface of gold afforded a multicomponent self-assembled monolayer (SAM) in which the differing tail groups were well mixed at the molecular level. The new "mixed" SAM was characterized by ellipsometry, contact angle goniometry, polarization modulation infrared reflection absorption spectroscopy (PM-IRRAS), and atomic force microscopy (AFM). Comparison of the new SAM to those generated by the coadsorption of mixtures of normal alkanethiols having analogous chain lengths and surface compositions showed that local domain formation (or "islanding") of the tail groups found in the latter SAMs was absent in the SAM derived from the unsymmetrical spiroalkanedithiol.

## Introduction

Much recent research involving organic thin films has targeted the preparation of well-defined multicomponent interfaces for use both in technological applications and as model systems for exploring the molecular-level basis for wetting,[1] adhesion,[2] corrosion resistance,[3] and lubrication.[4] Previous efforts to generate multicomponent organic interfaces that are homogeneously mixed at the molecular level have relied predominantly on the coadsorption of two or more organic compounds having different terminal functional groups and/or different chain lengths.[5−8] These efforts, however, have been hampered by the tendency of the adsorbates to form single-component domains or "islands" on the surface.[9−12] Other strategies have focused on the modification of preformed films (e.g., the preparation of interchain anhydrides followed by the reaction of alkylamines)[13] or the use of multicomponent adsorbates (e.g., unsymmetrical sulfides or disulfides).[14−16] These strategies also suffer from a variety of drawbacks, including incomplete amide formation for the interchain anhydrides,[13] disordered and weakly adsorbed films from the sulfides,[14,17] and S−S bond cleavage on the surface for the disulfides.[15,16]

Recently, we demonstrated the preparation of robust, conformationally ordered self-assembled monolayers (SAMs) from the adsorption of 2,2-dialkylpropane-1,3-dithiols or "spiroalkanedithiols" (C*n*C*m*$(SH)_2$, where $n = m$; Figure 1) onto the surface of gold.[18] In the present work, we target the use of a specifically designed unsymmetrical spiroalkanedithiol (C10C17-$(SH)_2$, where $n = 10$ and $m = 17$; Figure 1) for the purpose of generating a "mixed" SAM in which the two different alkyl groups are uniformly distributed at the molecular level. While this adsorbate might plausibly exhibit surface geometries comprised of (1) rows of long-long and short-short chains side by side or (2) nanometer-scale patches of long and short chain lengths distributed across the surface, we believed that the problem of micrometer-scale islanding[9−12] would be circumvented by tethering two different chains via a single carbon atom. Herein, we characterize this new "mixed" SAM by ellipsometry, contact angle goniometry, polarization modulation infrared reflection absorption spectroscopy (PM-IRRAS), and atomic force microscopy (AFM). Furthermore, we compare the properties of this SAM to those of the corresponding "mixed" SAMs generated by the adsorption of mixtures of *n*-decanethiol (*n*-C10SH) and *n*-heptadecanethiol (*n*-C17SH). Taken together, the results demonstrate that the adsorption of C10C17$(SH)_2$ onto gold affords the first unambiguous example of a two-component organic thin film in which the differing components are homogeneously mixed at the molecular level.

## Experimental Section

**Materials.** The sources of the materials and reagents have been largely described in a previous report.[18] Decanethiol was purchased

(1) Abbott, N. L.; Gorman, C. B.; Whitesides, G. M. *Langmuir* **1995**, *11*, 16.
(2) López, G. P.; Albers, M. W.; Schreiber, S. L.; Carrol, R.; Peralta, E.; Whitesides, G. M. *J. Am. Chem. Soc.* **1993**, *115*, 5877.
(3) Jennings, G. K.; Munro, J. C.; Yong, T.-H.; Laibinis, P. E. *Langmuir* **1998**, *14*, 6130.
(4) Carpick, R. W.; Salmeron, M. *Chem. Rev.* **1997**, *97*, 1163.
(5) Bain, C. D.; Evall, J.; Whitesides, G. M. *J. Am. Chem. Soc.* **1989**, *111*, 7155.
(6) Bain, C. D.; Whitesides, G. M. *J. Am. Chem. Soc.* **1989**, *111*, 7164.
(7) Folkers, J. P.; Laibinis, P. E.; Whitesides, G. M. *Langmuir* **1992**, *8*, 1330.
(8) Kang, J. F.; Liao, S.; Jordan, R.; Ulman, A. *J. Am. Chem. Soc.* **1998**, *120*, 9662.
(9) Folkers, J. P.; Laibinis, P. E.; Whitesides, G. M.; Deutch, J. *J. Phys. Chem.* **1994**, *98*, 563.
(10) Stranick, S. J.; Parikh, A. N.; Tao, Y.-T.; Allara, D. L.; Weiss, P. S. *J. Phys. Chem.* **1994**, *98*, 7636.
(11) Tamada, K.; Hara, M.; Sasabe, H.; Knoll, W. *Langmuir* **1997**, *13*, 1558.
(12) Frommer, J. *Angew. Chem., Int. Ed. Engl.* **1992**, *31*, 1298.
(13) Yan, L.; Marzolin, C.; Terfort, A.; Whitesides, G. M. *Langmuir* **1997**, *13*, 6704.
(14) Troughton, E. B.; Bain, C. D.; Whitesides, G. M.; Nuzzo, Allara, D. L.; Porter, M. D. *Langmuir* **1988**, *4*, 365.
(15) Biebuyck, H. A.; Whitesides, G. M. *Langmuir* **1993**, *9*, 1766.
(16) Ishida, T.; Yamamoto, S.; Mizutani, W.; Motomatsu, M.; Tokumoto, H.; Hokari, H.; Azehara, H.; Fujihira, M. *Langmuir* **1997**, *13*, 3261.
(17) Bain, C. D.; Troughton, E. B.; Tao, Y.-T.; Evall, J.; Whitesides, G. M.; Nuzzo, R. G. *J. Am. Chem. Soc.* **1989**, *111*, 321.
(18) Shon, Y.-S.; Lee, T. R. *Langmuir* **1999**, *15*, 1136.

10.1021/ja991987b CCC: $19.00 
Published on Web 02/01/2000

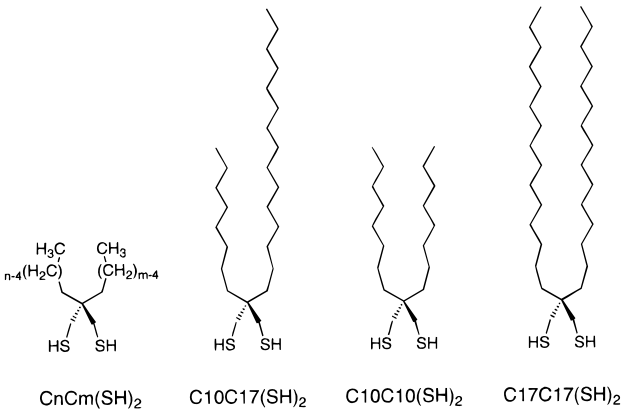


**Figure 1.** Structures of spiroalkanedithiols, C*n*C*m*$(SH)_2$, used to generate SAMs on gold.

from Aldrich Chemical Co., and heptadecanethiol was synthesized using unexceptional methods. Details of the synthesis of the 2,2-dialkylpropane-1,3-dithiols, C17C17$(SH)_2$ and C10C10$(SH)_2$, have been provided previously;[18] 2-octyl-2-pentadecylpropane-1,3-dithiol (C10C17$(SH)_2$) was prepared similarly. Complete analytical data are provided for this previously unreported adsorbate. $^1$H NMR (300 MHz, $CDCl_3$): $\delta$ 2.52 (d, $J = 9.3$ Hz, 4 H, SC*H*$_2$), 1.37−1.22 (m, 42 H), 1.08 (t, $J = 9.3$ Hz, 2 H, S*H*), 0.88 (t, $J = 7.7$ Hz, 6 H, C*H*$_3$). $^{13}$C NMR (75 MHz, $CDCl_3$): $\delta$ 39.8, 33.6, 31.9, 30.4, 30.3, 29.7−29.3 (m), 22.7, 14.1. Anal. Calcd for $C_{26}H_{54}S_2$: C, 72.48; H, 12.63. Found: C, 72.79; H, 12.45.

**Preparation of SAMs.** Methods for the preparation of evaporated Au/Si substrates have been described.[18] The Au(111) surfaces were formed by annealing a gold wire in a flame of $H_2/O_2$ to produce a number of atomically flat (111) terraces around the circumference of the resultant gold microball; detailed procedures for the preparation and characterization of these gold substrates have been described in a previous report.[19] All SAMs were generated by dipping the freshly prepared gold surfaces for 48 h in 1 mM solutions of the adsorbates in isooctane. The resultant SAMs were exhaustively rinsed with toluene and ethanol, and dried under a flow of ultrapure nitrogen before characterization.

**Characterization of SAMs.** The thicknesses of the films on the Au/Si substrates were measured using a Rudolf Research Auto EL III ellipsometer equipped with a He-Ne laser operating at a wavelength of 632.8 nm and an angle of incidence of 70°. Optical constants of the bare Au/Si substrates were collected immediately after the evaporation of gold. Ellipsometric measurements were averaged over three separate slides using three spots per slide for each type of SAM. A refractive index of 1.45 was assumed for all measurements.

Advancing contact angles of all liquids were measured on the Au/Si substrates at room temperature and ambient relative humidity using a ramé-hart model 100 contact angle goniometer. Contacting liquids were dispensed and withdrawn with a Matrix Technologies micro-Electrapette 25 operating at the slowest possible speed (ca. 1 $\mu$L/s) while maintaining constant contact between the pipet tip and the drop of liquid. The data were collected and averaged over three separate slides by depositing three drops on each slide and taking separate measurements from the opposite edges of each drop.

Polarization modulation infrared reflection absorption spectroscopy (PM-IRRAS) data were obtained using a Nicolet MAGNA-IR 860 Fourier transform spectrometer equipped with a liquid nitrogen-cooled mercury-cadmium-telluride (MCT) detector and a Hinds Instruments PEM-90 photoelastic modulator operating at 37 kHz. The polarized light was focused onto the Au/Si substrates at an angle of incidence of 80°. Spectral data were collected over 256 scans at a resolution of 4 $cm^{-1}$.

Topographic and frictional data for the SAMs on Au(111) were obtained by AFM utilizing conventional beam deflection techniques and a single tube scanner (0.5 in. in diameter and 1.0 in. in length).[19] Light from a laser diode was focused on the backside of the V-shaped microfabricated cantilever (Digital Instruments), which supported the probe tip ($SiN_3$) protruding from underneath. The sample was scanned relative to a fixed cantilever position. Deflections of the cantilever generated by interaction of the probe tip and the sample surface were detected by a four-quadrant position-sensitive detector. With this methodology, both normal and lateral deflections of the cantilever were simultaneously recorded. Sample positioning as well as data collection and processing were controlled by RHK AFM 100 and RHK STM 1000 electronics and software.

## Results and Discussion

First, we measured the ellipsometric thickness of the SAM generated from C10C17$(SH)_2$ and compared the data to those of the SAMs generated from C10C10$(SH)_2$ and C17C17$(SH)_2$ (see Figure 1). The data in Table 1 show that the ellipsometric thickness of the SAM generated from C10C17$(SH)_2$ is ~4 Å higher than that of C10C10$(SH)_2$ and ~6 Å lower than that of C17C17$(SH)_2$. That is, the thickness of the SAM derived from the unsymmetrical spiroalkanedithiol is intermediate between those of the SAMs derived from the symmetrical spiroalkanedithiols. Correspondingly, the average thicknesses of the SAMs derived from mixtures of *n*-C10SH and *n*-C17SH vary systematically with the molar ratio of the two thiols in solution (Table 1). When the solution ratio ($r_{sol}$ = [*n*-C10SH]/[*n*-C17SH]) is equal to 1, the thickness of the resulting SAM is comparable to that of the SAM derived solely from *n*-C17SH (±2 Å), which indicates the preferential adsorption of the long-chain thiol as reported previously.[6] Moreover, the thicknesses gradually decrease as the fraction of *n*-C10SH increases. The data further suggest that an equimolar surface concentration occurs when $r_{sol}$ ranges from 2 to 4. Within this range of solution ratios, the thicknesses of the "mixed" *n*-alkanethiolate SAMs correlate well with that of the "mixed" SAM generated from C10C17$(SH)_2$.

Second, we measured the advancing contact angles of water ($\theta_a^{H_2O}$) and hexadecane ($\theta_a^{HD}$) on these surfaces (Table 1). For all single component surfaces (i.e., those generated from C10C10$(SH)_2$, *n*-C10SH, C17C17$(SH)_2$, and *n*-C17SH), the advancing contact angles of water are indistinguishable ($\theta_a^{H_2O}$ = 113−114°). In contrast, however, the advancing contact angle of water for the SAM generated from C10C17$(SH)_2$ is significantly lower ($\theta_a^{H_2O}$ = 105°). Moreover, the advancing contact angles of water for the SAMs generated from mixtures of *n*-C10SH and *n*-C17SH exhibit the same low value ($\theta_a^{H_2O}$ = 105°) when $r_{sol}$ = 2−3. We note that for $r_{sol}$ = 2−3, both the water contact angles and the ellipsometric thicknesses are similar to those of SAMs generated from C10C17$(SH)_2$, suggesting similar surface compositions for both types of "mixed" SAMs. A similar conclusion can be drawn from the $\theta_a^{HD}$ data, which are particularly sensitive to small differences in the structure/composition of hydrocarbon interfaces.[20]

Third, we analyzed the vibrational spectra of the SAMs by PM-IRRAS. We focused on the frequency of the antisymmetric methylene C−H stretch ($\upsilon_a^{CH_2}$) because the position of this band can be used to evaluate the degree of conformational order (or crystallinity) of organic thin films.[21] As shown in Table 1 and Figure 2, the $\upsilon_a^{CH_2}$ band of the SAM generated from C10C17-$(SH)_2$ appears at a reproducibly higher frequency (2927 $cm^{-1}$) than those of the SAMs generated from either C10C10$(SH)_2$ or C17C17$(SH)_2$ (2925 or 2921 $cm^{-1}$, respectively), suggesting liquidlike chains for the SAMs generated from the unsymmetrical spiroalkanedithiol. Further comparison to the SAMs

(19) Kim, H. I.; Koini, T.; Lee, T. R.; Perry, S. S. *Langmuir* **1997**, *13*, 7192.

(20) Bain, C. D.; Whitesides, G. M. *Angew. Chem., Int. Ed. Engl.* **1989**, *1*, 506.

(21) Nuzzo, R. G.; Dubois, L. H.; Allara, D. L. *J. Am. Chem. Soc.* **1990**, *112*, 558.

**Table 1.** Ellipsometric Thicknesses, Advancing Contact Angles of Water ($H_2O$) and Hexadecane (HD), Wavenumbers of the Antisymmetric Methylene Bands ($\upsilon_a^{CH_2}$), and Frictional Responses (au) of the SAMs[a]

| adsorbate | thickness (Å) | $\theta_a^{H_2O}$ (deg) | $\theta_a^{HD}$ (deg) | $\upsilon_a^{CH_2}$ ($cm^{-1}$) | friction (au)[b] |
|---|---|---|---|---|---|
| C10C10$(SH)_2$ | $9 \pm 2$ | $113 \pm 1$ | $41 \pm 1$ | $2925 \pm 1$ | $5.0 \pm 0.3$ |
| *n*-decanethiol (*n*-C10SH) | $10 \pm 2$ | $113 \pm 1$ | $46 \pm 1$ | $2923 \pm 1$ | $4.3 \pm 0.4$ |
| C17C17$(SH)_2$ | $19 \pm 2$ | $114 \pm 1$ | $48 \pm 1$ | $2921 \pm 1$ | $2.8 \pm 0.3$ |
| *n*-heptadecanethiol (*n*-C17SH) | $19 \pm 2$ | $114 \pm 1$ | $47 \pm 1$ | $2919 \pm 1$ | $2.3 \pm 0.4$ |
| C10C17$(SH)_2$ | $13 \pm 1$ | $105 \pm 1$ | <10 | $2927 \pm 1$ | $9.2 \pm 0.3$ |
| [*n*-C10SH]/[*n*-C17SH] | | | | | |
| $r_{sol} = 1$ | $17 \pm 1$ | $108 \pm 1$ | $28 \pm 1$ | $2922 \pm 1$ | |
| $r_{sol} = 2$ | $14 \pm 1$ | $105 \pm 1$ | <10 | $2925 \pm 1$ | $3.3 \pm 0.2$ |
| $r_{sol} = 3$ | $13 \pm 2$ | $105 \pm 1$ | <10 | $2925 \pm 1$ | |
| $r_{sol} = 4$ | $13 \pm 2$ | $107 \pm 2$ | <10 | $2924 \pm 1$ | |
| $r_{sol} = 10$ | $11 \pm 1$ | $110 \pm 1$ | $18 \pm 1$ | $2923 \pm 1$ | |

[a] We report average values of thickness and wettability for at least nine independent measurements. Observed values were always within the indicated range. Values of $\upsilon_a^{CH_2}$ were similarly reproducible. [b] Standard deviations were obtained from the average of five independent measurements over 500 Å × 500 Å at a fixed load. While frictional data were not collected for all mixed SAMs, independent comparisons between $r_{sol} = 2$ and 3 gave indistinguishable results.

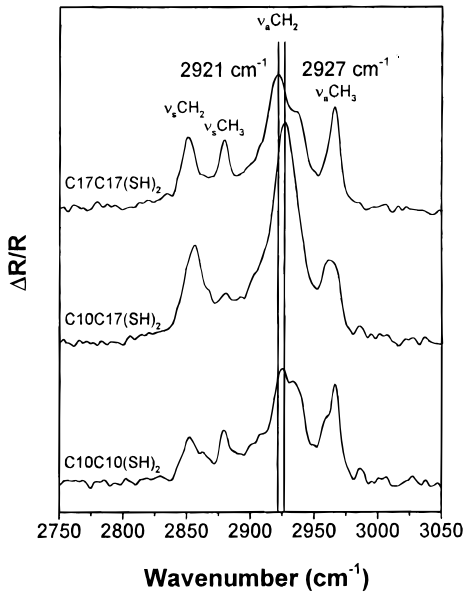


**Figure 2.** Surface infrared spectra (PM-IRRAS) of SAMs on gold derived from C17C17$(SH)_2$, C10C17$(SH)_2$, and C10C10$(SH)_2$. The position of the $\upsilon_a^{CH_2}$ band ranges from a minimum of 2921 $cm^{-1}$ for C17C17$(SH)_2$ to a maximum of 2927 $cm^{-1}$ for C10C17$(SH)_2$. The differential surface reflectivity ($\Delta R/R$) was calculated as the ratio $(R_p - R_s)/(R_p + R_s)$, where $R_p$ and $R_s$ represent the reflectivity for the respective polarizations of light.

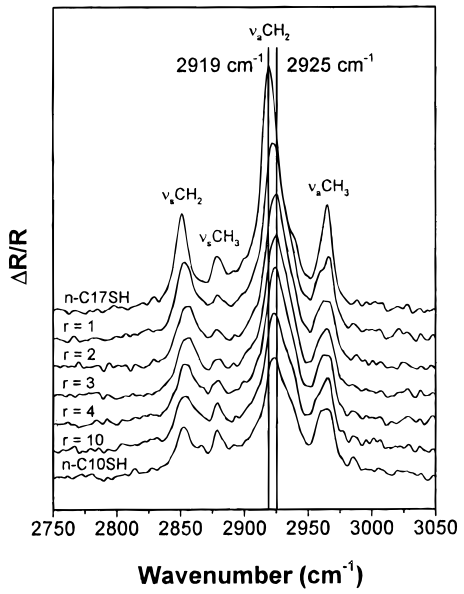


**Figure 3.** Surface infrared spectra (PM-IRRAS) of SAMs on gold derived from mixtures of *n*-C10SH and *n*-C17SH (where $r_{sol} = 1-10$). The position of the $\upsilon_a^{CH_2}$ band ranges from a minimum of 2919 $cm^{-1}$ for *n*-C17SH to a maximum of 2925 $cm^{-1}$ for $r_{sol} = 2$ and 3. The differential surface reflectivity ($\Delta R/R$) was calculated as the ratio $(R_p - R_s)/(R_p + R_s)$,, where $R_p$ and $R_s$ represent the reflectivity for the respective polarizations of light.

generated from *n*-alkanethiols reveals that the SAMs generated from C10C10$(SH)_2$ and C17C17$(SH)_2$ are slightly less crystalline than those generated from *n*-C10SH and *n*-C17SH, respectively. We reported this difference in our previous study of spiroalkanedithiol SAMs,[18] and proposed that the difference arises from disorder introduced by the tetrahedral geometry of the quaternary carbon atom. The frequency of the $\upsilon_a^{CH_2}$ band of the SAMs derived from mixtures of *n*-C10SH and *n*-C17SH increases to a maximum value of 2925 $cm^{-1}$ when $r_{sol} = 2-3$ (Table 1 and Figure 3). This observation provides further support that the interfaces generated from C10C17$(SH)_2$ and those generated from mixtures of *n*-C10SH and *n*-C17SH (where $r_{sol} = 2-3$) have similar chemical compositions.

Fourth, to provide a more local evaluation of the surface structure,[18] we examined the SAMs by AFM. This technique probes the topography and frictional response of interfaces on a truly molecular scale, and thus serves as a useful tool to analyze the size, order,[22] and distribution of molecular islands.[11,12] Using well-defined Au(111) substrates,[19] we compared the topographies and frictional properties of SAMs generated from the spiroalkanedithiols (C10C10$(SH)_2$, C17C17$(SH)_2$, and C10C17$(SH)_2$) to those of the corresponding SAMs generated from *n*-C10SH, *n*-C17SH, and a mixed solution of *n*-C10SH and *n*-C17SH, where $r_{sol} = 2$. Figure 4 shows representative topographic images (500 Å × 500 Å) and line plots of the six SAMs. At this scale, all topographic images are largely featureless, and the corresponding root-mean-square roughnesses are generally similar except for those of the SAM derived from the mixture of *n*-alkanethiols. We interpret these topographic images to reflect islanding in only the latter "mixed" SAM. In addition, the average height difference between red and blue areas in the latter topographic image is ~8 Å, which is consistent with the expected height difference between *n*-heptadecanethiol and *n*-decanethiol SAMs on gold (~7.7 Å).[23]

(22) Xiao, X.; Hu, J.; Charych, D. H.; Salmeron, M. *Langmuir* **1996**, *12*, 235. Lio, A.; Charych, D. H.; Salmeron, M. *J. Phys. Chem. B* **1997**, *101*, 3800.

(23) Porter, M. D.; Bright, T. B.; Allara, D. L.; Chidsey, C. E. D. *J. Am. Chem. Soc.* **1987**, *109*, 3559.

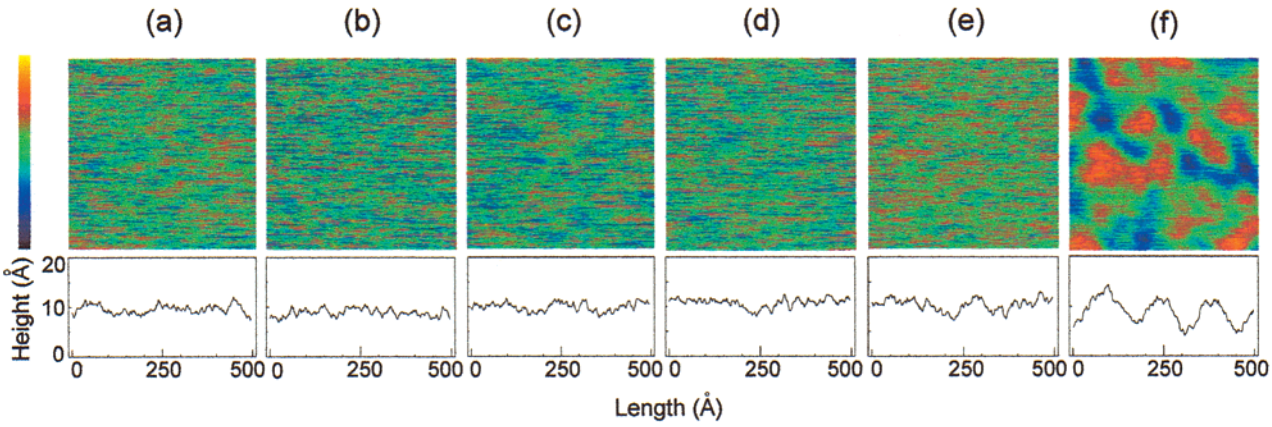


**Figure 4.** Topographic AFM images of the SAMs derived from (a) C10C10(SH)$_2$, (b) *n*-C10SH, (c) C17C17(SH)$_2$, (d) *n*-C17SH, (e) C10C17(SH)$_2$, and (f) a mixture of *n*-C10SH and *n*-C17SH, where $r_{sol} = 2$. In these images, red corresponds to topographic highs and blue corresponds to topographic lows. Line plots of the corresponding topographic heights across the center of each image are also provided. The observed trends were reproducible on at least five independently prepared samples.

The corresponding measurements of friction by AFM provided further insight into the nanoscale structure and order of the films. We observed homogeneous frictional responses on all SAMs except for that derived from the mixture of *n*-alkanethiols; for this SAM, we observed a slight contrast in the frictional response of the different islands (data not shown).[24] Moreover, the data in Table 1 show that the average frictional response of the latter SAM is intermediate between those of the SAMs formed separately from the two *n*-alkanethiols, which is again consistent with separate islands of the two components within this film. If the two *n*-alkanethiolate moieties were homogeneously mixed on the surface, we would have predicted a frictional response higher than that observed on either single-component *n*-alkanethiol SAM because of the liquidlike nature of the two-component SAM (as indicated above from the PM-IRRAS data), given that previous studies have shown that the frictional responses of organic thin films are greater for liquidlike films than for crystalline films.[22,24,25]

Correspondingly, we note that the frictional response of the "mixed" SAM derived from C10C17(SH)$_2$ is substantially higher than that observed for the mixed SAM derived from the mixture of *n*-alkanethiols and that observed on the SAMs derived separately from C10C10(SH)$_2$ and C17C17(SH)$_2$. We propose that the higher frictional response for the C10C17(SH)$_2$ SAM arises from enhanced interactions between the AFM tip and the homogeneous liquidlike film. These interactions probably arise from the protrusion of the loosely packed C17 tail, which affords enhanced van der Waals contact with the tip and/or increased film deformation during sliding.

## Conclusions

We have demonstrated that unsymmetrical spiroalkanedithiols can be used to generate two-component SAMs on gold in which the different alkyl chains are homogeneously mixed at the molecular level. The structural design of these adsorbates circumvents the possibility of molecular islanding, which occurs when analogous "mixed" SAMs are generated by the coadsorption of mixtures of *n*-alkanethiols. We anticipate that the new homogeneously "mixed" SAMs will provide useful model systems for the study of interfacial phenomena.[26] We are currently investigating, for example, the influence of nanoscale roughness on the wettability and frictional properties of organic thin films derived from these adsorbates.

**Acknowledgment.** The National Science Foundation (Grants DMR-9700662 and CAREER Award to TRL: CHE-9625003) and the Robert A. Welch Foundation (Grant No. E-1320) provided generous support for this research.

JA991987B

(24) Previous studies by AFM have shown that SAMs having longer alkyl chains exhibit lower frictional responses than those having shorter alkyl chains: McDermott, M. T.; Green, J.-B.; Porter, M. D. *Langmuir* **1997**, *13*, 2504, and ref 22.

(25) Additional support for islanding in the "mixed" *n*-alkanethiol SAM lies in our observation of an inverse relationship between topography and frictional response (as noted in the text). The observed inverse relationship is consistent with the known correlation between chain length (i.e., conformational order) and frictional response in SAMs.[22,24]

(26) For example, the similar wettabilities for the C10C17(SH)$_2$ SAM and the islanded SAMs (where $r_{sol} = 2-4$) suggest that nanoscopic island boundaries exert a surprisingly strong influence upon macroscopic wettability. Future studies will address this hypothesis.